

Combating Distribution Shift for Accurate Time Series Forecasting via Hypernetworks

1st Wenyang Duan

School of Mathematics and Computer Sciences
Nanchang University
Nanchang, China
wenyangduan@ncu.edu.cn

2nd Xiaoxi He

Computer Engineering and Networks Laboratory
ETH Zurich
Zurich, Switzerland
hex@ethz.ch

3rd Lu Zhou

Department of Civil and Environmental Engineering
The Hong Kong Polytechnic University
HongKong
lu.lz.zhou@polyu.edu.hk

4th Lothar Thiele

Computer Engineering and Networks Laboratory
Zurich, Switzerland
Zurich, Switzerland
thiele@ethz.ch

5th Hong Rao*

school of software
Nanchang University
Nanchang, China
raohong@ncu.edu.cn

arXiv:2202.10808v2 [cs.LG] 14 Jul 2022

Abstract—Time series forecasting has widespread applications in urban life ranging from air quality monitoring to traffic analysis. However, accurate time series forecasting is challenging because real-world time series suffer from the distribution shift problem, where their statistical properties change over time. Despite extensive solutions to distribution shifts in domain adaptation or generalization, they fail to function effectively in unknown, constantly-changing distribution shifts, which are common in time series. In this paper, we propose Hyper Time-Series Forecasting (HTSF), a hypernetwork-based framework for accurate time series forecasting under distribution shift. HTSF jointly learns the time-varying distributions and the corresponding forecasting models in an end-to-end fashion. Specifically, HTSF exploits the hyper layers to learn the best characterization of the distribution shifts, generating the model parameters for the main layers to make accurate predictions. We implement HTSF as an extensible framework that can incorporate diverse time series forecasting models such as RNNs and Transformers. Extensive experiments on 9 benchmarks demonstrate that HTSF achieves state-of-the-art performances.

Index Terms—hypernetworks, time series forecasting, distribution shift

I. INTRODUCTION

Time-series forecasting is crucial for various data analytics domains, including air quality monitoring [1], renewable energy production [2], human activity recognition [3], electricity consumption planning [4], urban traffic analysis [4] etc. The past years have witnessed diverse time-series forecasting models ranging from the conventional statistical approaches *e.g.*, auto-regressive integrated moving average (ARIMA) [5] to the more recent deep learning based models such as recurrent neural networks (RNNs) [6], transformers, [7] and their variants [4], [8]–[10]. As deep learning based models make few assumptions on the temporal structures of time series, they are preferable in modeling complex, long-sequence time series. They have demonstrated a notable improvement in prediction accuracy than statistical models [8].

*Corresponding Author

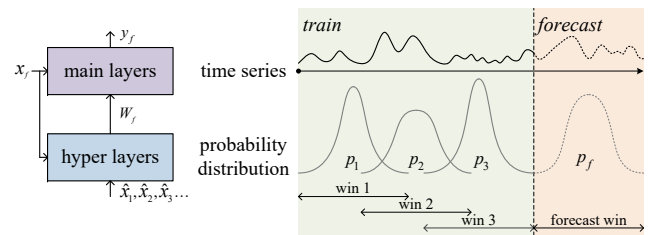


Fig. 1. Illustration of distribution shifts in time series forecasting and our solution. Given sliding windows win 1, 2, 3 and so on, the data distributions p_1, p_2, p_3, \dots vary across windows, and they are likely to differ from the distribution p_f in the forecasting window. Our solution is to explicitly model and learn the data distributions from the historical sequences $\hat{x}_1, \hat{x}_2, \hat{x}_3, \dots$ via hyper layers, which generate the model parameters W_f for the main layers. The main layers then take x_f as input and generate the predictions y_f .

A unique challenge in time series forecasting is that they are often non-stationary, resulting in temporal shifts in their distributions. This distribution shift phenomenon causes discrepancies between the distributions of the training and the testing data, which degrades the performance of forecasting models [11], [12]. Such distribution shift also exists among the input sequences of the training data, which makes it challenging to train a model that generalizes well to unknown data [13], [14]. Figure 1 illustrates the distribution shift problem in time series forecasting. Consider three sliding windows 1, 2, and 3 to segment the time series for training. The probability distributions of the time series p_1, p_2, p_3 may vary across windows, and they are likely to differ from the distribution p_f in the unseen forecast window. That is, $p_1 \neq p_2 \neq p_3 \neq p_f$, which makes accurate forecasting for window p_f challenging.

Distribution shift is usually tackled by domain generalization [15] or domain adaptation [14], [16]. The idea is to learn the common knowledge transferable between domains despite the differences in their distributions [15]. However, it is non-

trivial to apply these techniques to time series [12], [17]. This is because the distributions in time series change constantly (e.g., p_1, p_2, p_3 in Figure 1), and it is unknown *how to best characterize the distributions* upon which to learn the common knowledge [12]. The state-of-the-art, ADARNN [12] proposes to characterize the *worst-case* distribution shift in time series leveraging the principle of maximum entropy. Nevertheless, this approach is sub-optimal because (i) the training data may not always contain the worst-case distribution shift; and (ii) it under-utilizes the diversity of the distribution shifts in the time series.

In this paper, we propose a hypernetwork-based framework called Hyper Time-Series Forecasting (HTSF) to mitigate the distribution shift problem for accurate time series forecasting. The idea is to jointly learn the common knowledge and the corresponding distributions with an end-to-end hypernetwork architecture. As shown in Figure 1, a hypernetwork consists of hyper and main layers, where the hyper layers generate model parameters W_f conditioned on the inputs \mathbf{x}_f for the main layers to make predictions y_f . We exploit the hyper layers to learn the best characterization of the distribution shifts and the main layers to learn the corresponding forecast model. Our strategy is advantageous in the following aspects. (i) The end-to-end learning scheme eliminates the assumptions on the worst-case distribution shift in the training data and makes full use of the various distribution shifts in the training data. (ii) The hypernetwork architecture is capable of modeling complex feature representations in both the distributions and the common transferable knowledge, and it applies to various deep learning based time series models.

Our main contributions are summarized as follows:

- We propose HTSF, a hypernetwork-based framework for accurate time series forecasting. To the best of our knowledge, it is the first study that addresses the distribution shift problem in time series via hypernetworks.
- HTSF offers a generic, extensible, and end-to-end solution to the distribution shift problem in time series that makes no assumptions on the training data and applies to diverse deep learning based time series models such as RNNs and transformers.
- We evaluate HTSF on 9 time series forecasting benchmarks. Experimental results show that HTSF achieves state-of-the-art accuracy in both short-term and long-term time series forecasting. It also yields comparable performance on spatiotemporal data to the state-of-the-art graph neural network based solutions [18], [19].

In the rest of this paper, we review related work in Sec. II, present the problem statement in Sec. III and introduce our method in Sec. IV. We report the performance in Sec. V and ablation studies in Sec. VI, and finally conclude in Sec. VII.

II. RELATED WORK

Our work is related to the following categories of research.

A. Time Series Forecasting

For time series forecasting, we distinguish between statistic models and deep learning based models. Statistic models [20], [21] are interpretable and theoretically sound. But they often suffer from heavy crafting on data pre-processing and labor-intensive feature engineering, which may fail to capture complex patterns in time series. Recently, deep learning based models have attracted increasing attention due to their outstanding performance in time series analysis. For example, RNN-based models [2], [8], [22] prove effective in capturing both short-term and long-term patterns. Transformer-based models [4], [23] have shown remarkable performance for extremely long sequences. However, they are not robust to the distribution shift problem and suffer from performance degradation [12], [17].

B. Distribution Shift

Domain adaptation [14], [16] and domain generalization [15] are generic solutions to the distribution shift problem. Domain adaptation focuses on the disparity difference between the source and target domain, whereas domain generalization aims to learn a generalizable model from various source domains. However, it is non-trivial to apply these techniques to time series. For example, some research reports [24] that domain adversarial learning, a prevailing domain adaptation technique, may be inappropriate for regression, while time series forecasting is often a regression task. Furthermore, since the distributions in time series change constantly, it is not straightforward how to define multiple source domains in non-stationary time series [12].

A few pioneer studies [12], [17] explore solving the distribution shift problem in time series forecasting. RevIN [17] proposes an instance-level normalization technique to reduce the discrepancy in data distributions such as mean and variance. Our work is orthogonal to RevIN by adopting representation learning to enhance the generalization of forecasting models. Our work is most related to ADARNN [12], which first attempts to characterize the worst-case distribution shift in time series and then matches the distributions to learn a generalizable model. We advance ADARNN by eliminating the worst-case assumption and fully exploiting the diversity of the distribution shifts in the training data.

C. Hypernetworks

A hypernetwork [25] utilizes a primary neural network g to generate weights θ_f for a second network f . The network f with the weights θ_f can then be applied for specific inference tasks. Hypernetworks have demonstrated superior performances on many benchmarks [26], [27], due to their ability to adapt f for different inputs, which allows the hypernetwork to model tasks more effectively [28]. Hypernetworks have been applied in few-shot learning [29], continual learning [27], efficient parameter fine-tuning [30], [31] etc. A few studies have also introduced hypernetworks in time series forecasting such as traffic prediction [32]. However, it does not explicitly account for the distribution shift problem, and thus results in

sub-optimal accuracy. To the best of our knowledge, we are the first to adopt hypernetworks to tackle the distribution shift problem in time series forecasting.

III. PROBLEM STATEMENT

We consider a standard multi-variate time series forecasting problem as follows. A time series \mathcal{X} with the corresponding label sequence \mathcal{Y} , is segmented into a set of sequences with labels $\mathcal{D} = \{\mathbf{x}^{(i)}, \mathbf{y}^{(i)}\}_i^N$, where $\mathbf{x}^{(i)} \in \mathbb{R}^{d_x \times T_x}$ is a sub-sequence of \mathcal{X} , $\mathbf{y}^{(i)} \in \mathbb{R}^{d_y \times T_y}$ is the corresponding label form \mathcal{Y} . N , d_x , d_y , T_x , and T_y denote the number of sequences, the dimension of input variables, the dimension of label variables, the input length and the prediction length, respectively. Our objective is to learn a model $\mathcal{M} : \mathbf{x}_i \rightarrow y_i$ from \mathcal{D}_{train} for unseen sequences in \mathcal{D}_{test} , where \mathcal{D}_{train} and \mathcal{D}_{test} are the training and test sets from \mathcal{D} .

We aim to learn model \mathcal{M} in presence of *distribution shift* in the time series, which is described by the following assumptions.

- There is discrepancy between the marginal probability distribution $P_{\mathcal{D}_{train}}$ of the training set and the distribution $P_{\mathcal{D}_{test}}$ of the test set, *i.e.*, $P_{\mathcal{D}_{train}} \neq P_{\mathcal{D}_{test}}$. Note that $P_{\mathcal{D}_{train}}(Y|X) = P_{\mathcal{D}_{test}}(Y|X)$ because the underlying laws governing the inputs and the outputs of the time series usually stay the same [12].
- The marginal probability distribution of each $\mathbf{x}^{(i)}$ from \mathcal{D}_{train} may differ, although their conditional distributions are the same. That is $P_{\mathcal{D}}(\mathbf{x}^{(i)}) \neq P_{\mathcal{D}}(\mathbf{x}^{(j)})$, $1 \leq i \neq j \leq N$, $P_{\mathcal{D}}(\mathbf{y}^{(i)} | \mathbf{x}^{(i)}) = P_{\mathcal{D}}(\mathbf{y}^{(j)} | \mathbf{x}^{(j)})$.

The discrepancy between the training and test set highlights the necessity to account for distribution shift for accurate predictions, while that among the sub-sequences within the training set explains the challenges of effectively learning the model \mathcal{M} .

IV. METHOD

This section presents HTSF, our hypernetwork-based framework for time series forecasting under distribution shift. HTSF is a model-agnostic framework that can incorporate various deep learning based time series forecasting models such as RNNs and Transformers. For ease of presentation, we explain HTSF using a gated recurrent unit (GRU) as an example forecasting model.

A. HTSF Overview

Figure 2 depicts the overview of HTSF with GRUs as the underlying forecasting model, which we call HyperGRU. It mainly consists of two modules.

- *Hyper Layers*: These layers learn to characterize the distributions from the historical sequences. The learned distribution characterizations are then used to generate the weights of the main layers. We employ bidirectional GRU (BiGRU) for the hyper layers (see Sec. IV-B).
- *Main Layers*: These layers adapt their weights according to the learned distribution characterizations from the hyper layers as well as their own internal states through

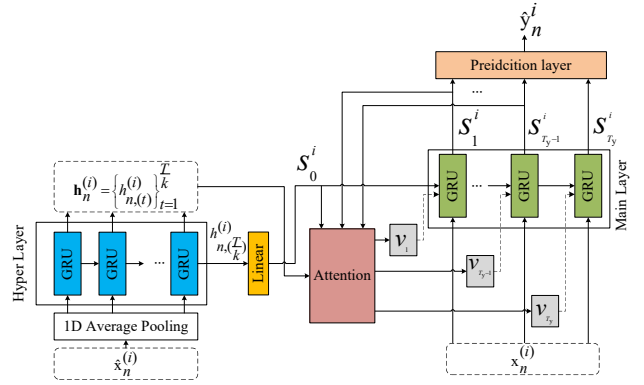


Fig. 2. An overview of HTSF, where we employ GRUs as the example forecasting model. The corresponding hypernetwork is termed HyperGRU.

an attention mechanism. As a result, the main layers can leverage the common knowledge extracted from the diverse distribution shifts to make accurate predictions. The core part of the main layers is a simple GRU cell (see Sec. IV-C).

The hyper and main layers of HyperGRU interact as follows. Let $\hat{\mathcal{X}}^{(i)}$ be the historical data of $\mathbf{x}^{(i)}$. $S = \{\hat{\mathbf{x}}_n^{(i)}\}_{n=1}^L$ is the historical dataset generated by $\hat{\mathcal{X}}^{(i)}$ with a sliding window of a fixed length T , where $\hat{\mathbf{x}}_n^{(i)} \in \mathbb{R}^{d_x \times T}$, $L = |\hat{\mathcal{X}}^{(i)}| - T + 1$. The hyper layers take all $\hat{\mathbf{x}}_n^{(i)}$ from S as inputs and output a set of representations of the historical marginal probability distributions. These representations and input at the current time step from $\mathbf{x}^{(i)}$ are then combined through the attention mechanism to generate the weights for the main layers at the next time step. Finally, the main layers make predictions as conventional time series forecasting methods.

Note that our method makes full use of the various distribution shifts in historical data S and aggregates the common transferable knowledge from S to mitigate the distribution shift problem for accurate time series forecasting. In comparison, prior proposals either ignore the distribution shift problem [4], [8], [9] or under-utilize the diverse distribution shifts in the time series [12].

B. Hyper Layers

The hyper layers are responsible to learn the complex feature representations of various distribution shifts. We use BiGRU to collectively encode all sequences in the historical data $S = \{\hat{\mathbf{x}}_n^{(i)}\}_{n=1}^L$.

- We first apply an 1D average pooling with kernel size k and stride k over $\hat{\mathbf{x}}_n^{(i)}$ on time dimension to down sample $\hat{\mathbf{x}}_n^{(i)}$ into its $\frac{1}{k}$ slice:

$$\bar{\mathbf{x}}_n^{(i)} = \text{AvgPool1D}(\hat{\mathbf{x}}_n^{(i)}) \quad (1)$$

where $\bar{\mathbf{x}}_n^{(i)} \in \mathbb{R}^{d_x \times \frac{T}{k}}$. Equ. (1) reduces the memory usage while preserving most of the information in the historical data [4]. We empirically show that such down-sampling has little impact on the prediction accuracy (see Sec. ??).

- Then we feed $\bar{\mathbf{x}}_n^{(i)}$ into a biGRU to generate the state sequence $\mathbf{h}_n^{(i)} \in \mathbb{R}^{\frac{T}{k} \times d_h}$:

$$\mathbf{h}_n^{(i)} = \left\{ h_{n,(t)}^{(i)} \right\}_{t=1}^{\frac{T}{k}} = \text{BiGRU} \left(\bar{\mathbf{x}}_n^{(i)} \right) \quad (2)$$

where $h_{n,(t)}^{(i)} \in \mathbb{R}^{d_h}$ is a hidden state with feature dimension d_h . Note that $\mathbf{h}_n^{(i)}$ can be considered as the distribution characterization for $\bar{\mathbf{x}}_n^{(i)}$.

The hyper layer explicitly models and characterizes the distributions from the historical data. Such information is then utilized to generate the weights of the main layers, as explained below.

C. Main Layers

The main layers can adaptively change their parameters conditioned on $\mathbf{h}_n^{(i)}$ and \mathbf{x}^i . The core part of a main layer is a simple GRU cell. To illustrate its weights generation process, we first present the standard formulation of the GRU cell:

$$\begin{aligned} r_t &= \sigma \left(W_{xr} x_t^{(i)} + W_{hr} s_{t-1}^{(i)} + b_r \right) \\ z_t &= \sigma \left(W_{xz} x_t^{(i)} + W_{hz} s_{t-1}^{(i)} + b_z \right) \\ n_t &= \tanh \left(W_{xn} x_t^{(i)} + r_t \odot \left(W_{hn} s_{t-1}^{(i)} + b_n \right) \right) \\ s_t^{(i)} &= (1 - z_t) \odot n_t + z_t \odot s_{t-1}^{(i)} \end{aligned} \quad (3)$$

where $x_t^{(i)} \in \mathbb{R}^{d_x}$ denotes input of the GRU cell from $\mathbf{x}^{(i)}$ at time step t , $s_t^{(i)} \in \mathbb{R}^{d_s}$ is the hidden state at t , σ is sigmoid function, W_{xr} , W_{xz} , W_{xn} , W_{hr} , W_{hz} , W_{hn} , b_r , b_z and b_n are learnable parameters.

The initial hidden state $s_0^{(i)}$ is computed as follows:

$$s_0^{(i)} = W_{init} h_{n,(\frac{T}{k})}^{(i)} + b_{init} \quad (4)$$

where $h_{n,(\frac{T}{k})}^{(i)}$ is the last state in $\mathbf{h}_n^{(i)}$; W_{init} and b_{init} are learnable parameters.

The weights of the GRU cell at current time step t are controlled by a vector v_t that varies dynamically with t :

$$W_{Ih} = W_{hv} v_t, W_{Ix} = W_{xv} v_t, W_{Ib} = W_{bv} v_t \quad (5)$$

where W_{hv} , W_{xv} and W_{bv} are learnable parameters. $W_{Ih} \in \mathbb{R}^{d_{Ih}}$, $W_{Ix} \in \mathbb{R}^{d_{Ix}}$, and $W_{Ib} \in \mathbb{R}^{d_{Ib}}$ are the weights of the GRU cell, v^t is determined by the previous state $s_{t-1}^{(i)}$ and the outputs of the hyper layers $\mathbf{h}_n^{(i)}$, which is computed by the attention mechanism:

$$v_t = W_c c_t, c_t = \sum_{p=1}^{\frac{T}{k}} \alpha_p h_{n,(p)}^{(i)}, \alpha_p = \frac{\exp \left(\text{score} \left(s_{t-1}^{(i)}, h_{n,(p)}^{(i)} \right) \right)}{\sum_{q=1}^{\frac{T}{k}} \exp \left(\text{score} \left(s_{t-1}^{(i)}, h_{n,(q)}^{(i)} \right) \right)} \quad (6)$$

where $\text{score}(\cdot)$ is a score function, according to Luong attention [33]. The score function is given by:

$$\text{score} \left(s_{t-1}^{(i)}, h_{n,(p)}^{(i)} \right) = V^T \tanh \left(W_s s_{t-1}^{(i)} + W_h h_{n,(p)}^{(i)} + b_s \right) \quad (7)$$

where V , W_s , W_h , and b_s are learnable parameters.

As mentioned above, all the parameters of the main layer are generated by W_{Ih} , W_{Ix} , and W_{Ib} :

$$\begin{aligned} (W_{hr}, W_{hz}, W_{hn}) &= \text{Chunk} (W_{Ih}) \\ (W_{xr}, W_{xz}, W_{xn}) &= \text{Chunk} (W_{Ix}) \\ (b_r, b_z, b_n) &= \text{Chunk} (W_{Ib}) \end{aligned} \quad (8)$$

where W_{hr} , W_{hz} , $W_{hn} \in \mathbb{R}^{d_s \times d_s}$, $d_s \times 3d_s = d_{Ih}$ and W_{xr} , W_{xz} , $W_{xn} \in \mathbb{R}^{d_s \times d_x}$, $d_s \times 3d_x = d_{Ix}$ and b_r , b_z , $b_n \in \mathbb{R}^{d_s}$, $3d_s = d_{Ib}$. $\text{Chunk}(\cdot)$ is the operation to split a tensor into a specific number of equal-sized chunks. Through Equ. (6), we can adaptively attach different information in $\mathbf{h}_n^{(i)}$ to the state of the GRU cell at the current time step t to dynamically adjust the weights of the main layers. By integrating Equ. (3), Equ. (5) and Equ. (6), we can dynamically generate weights of the main layers.

D. Training

According to Sec. IV-B and Sec. IV-C, we implement HyperGRU with a simple prediction layer (e.g., sigmoid function) that takes $\hat{\mathbf{x}}_n^{(i)}$ and $\mathbf{x}^{(i)}$ as inputs and outputs the prediction:

$$\hat{\mathbf{y}}_n^{(i)} = \text{HyperGRU}(\mathbf{x}^{(i)}, \hat{\mathbf{x}}_n^{(i)}) \quad (9)$$

The loss of the i -th pair $(\mathbf{x}^{(i)}, \mathbf{y}^{(i)})$ is calculated as follows:

$$\mathcal{L}_{\text{pred}}(\theta) = \frac{1}{L} \sum_{n=1}^L \text{criterion}(\hat{\mathbf{y}}_n^{(i)}, \mathbf{y}^i) \quad (10)$$

where $\text{criterion}(\cdot, \cdot)$ is an objective function, and θ denotes the learnable parameters of HyperGRU. Then we perform training using Equ. (10).

E. Extensions to Other Models

As mentioned, HTSF is a model-agnostic framework that can incorporate various time series forecasting models. We briefly explain how to extend HTSF to other RNNs such as vanilla RNN, LSTM [34], ConvLSTM [35] *et al.*

Extending HTSF to other RNNs is very straightforward. Take the LSTM as an example, we can use Equ. (6) to calculate v_t , and use v_t to generate the weights of memory cell, input gate, forget gate and output gate. The weights of other RNNs can be generated in a similar way.

V. EXPERIMENTS

In this section, we evaluate the performance of HTSF on 9 benchmarks and different time series models covering short sequence time series forecasting (Sec. V-A), grid-based spatiotemporal data forecasting (Sec. V-B), and graph-based data spatiotemporal forecasting (Sec. V-C). All experiments were conducted out on a single Nvidia RTX3090 GPU.

A. Short Sequence Time Series Forecasting

We test HTSF for short sequence time series forecasting on three datasets from diverse application domains.

TABLE I
DATASETS FOR SHORT SEQUENCE TIME SERIES FORECASTING.

Datasets	#Train	#Valid	#Test
Air quality	29,232	2,904	2,832
Electricity consumption	1,235,964	413,280	413,202
Human activity	6,000	1,352	2,947

1) Datasets and Metrics:

- **Air Quality** [1]: This dataset contains hourly air quality data collected from 12 stations in Beijing, China, from March 2013 to February 2017. We use data from the same four stations (Dongsi, Tiantan, Nongzhanguan, and Dingling) and the same six features (PM2.5, PM10, SO₂, NO₂, CO, and O₃) as [12]. We use the data from 01/03/2013 to 30/06/2016 for training, data from 01/07/2016 to 31/10/2016 for validation, and data from 02/11/2016 to 28/02/2017 for testing. The Root Mean Square Error (RMSE) and Mean Absolute Error (MAE) are used as the performance metrics.
- **Electricity Consumption** [36]: This dataset contains household electric power consumption measurements of 2, 062, 346 valid samples (null values removed). The measurements were collected between 16/12/2006 and 26/11/2010. Each interval lasts 10 min. We use the data from 16/12/2006 to 24/04/2009 for training, data from 25/02/2010 to 26/11/2010 for testing, and the remaining for validation. RMSE is used as the performance metric.
- **Human Activity** [3]: This dataset contains smartphone sensor data (accelerometer, gyroscope, and magnetometer) collected from 30 volunteers performing six activities. We predict the activities of volunteers based on the historical data. We use 7,352 instances for training and 2, 947 instances for testing following [12]. We use Accuracy (ACC), Precision (P), Recall (R), and F1 as the performance metrics.

2) *Baselines and Configurations*: We adopt GRU/LSTM as the hyper layers and main layers for our HTSF framework because they suffice for short sequence prediction in many applications [10], [18]. The corresponding models are termed HyperGRU and HyperLSTM. We compare them with the following baselines:

- **LSTM** : a standard long short memory network.
- **GRU** : a standard gated recurrent unit.
- **LightGBM** : a lightweight and efficient gradient boosting decision tree.
- **MMD-RNN** : a domain generalization method, whose backbone is changed to RNNs and uses maximum mean discrepancy measure as the final output of the RNN layers.
- **DANN-RNN** : the RNN version of a dynamic adversarial adaptation network to dynamically learn domain-invariant representations [12].
- **LSTNet** : a method combining Convolutional Neural Networks(CNNs) and LSTM for time series forecasting.

- **STRIPE** : an Encoder-Decoder model with a diversification mechanism from a determinantal point process.
- **ADARNN** : the state-of-the-art model to handle distribution shift in time series forecasting.

These baselines are chosen for the following reasons. LSTM and GRU are basic models in our HyperLSTM and HyperGRU. LightGBM is a popular and strong traditional machine learning algorithm in Kaggle competitions. LSTNet and STRIPE are state-of-the-art RNN-based methods without considering the problem of distribution shift. MMR-RNN, DANN-RNN, and ADARNN are recent models attempting to solve the distribution shift problem in time series, where ADARNN is state-of-the-art.

For all datasets, we use Adam [37] with weight decay regularization as the optimizer. The dataset-specific configurations are summarized below.

- **Air Quality**: We use L2 loss as the training objective. The learning rate is $2e-4$ with a weight decay of 0.01, and the batch size is 128. We set sliding window size $T = 672$ (28 consecutive days), $k = 24$ for 1D average pooling.
- **Electricity Consumption**: We use L2 loss as the training objective and $5e-5$ as the learning rate. We set sliding window size $T = 1008$ (one week), $k = 36$ for 1D average pooling, and the batch size is set to 64.
- **Human Activity**: We use cross-entropy as the training objective and the learning rate is $2e-5$ with a weight decay of 0.01. We set sliding window size $T = 128$, $k = 36$ for 1D average pooling, and the batch size is set to 256.

We set the prediction step $T_y = 1$ for all benchmarks as in [12].

3) *Results*: The left part of Table II shows the RMSE and MAE of different methods for the air quality prediction tasks. The right part of Table II presents the RMSE of predicting the power consumption. Table III lists the ACC, P, R, and F1 scores of different methods of activity classification. Since LSTNet and STRIPE are built for regression tasks, they are not applicable to this dataset. We make the following observations.

- HyperLSTM outperforms LSTNet and STRIPE, the methods that ignore distribution shift, by decreasing the RMSE/MAE by 61.4%/80.6% and 23.9% /34.4% in average. This indicates the importance of addressing the distribution shift problem.
- HyperLSTM and HyperGRU outperform MMD-RNN and DANN-RNN on all benchmarks, suggesting that HTSF better handles distribution shift than existing domain adaptation and generalization methods for time series forecasting.
- Compared to ADARNN, one state-of-the-art method for handling distribution shift, HyperLSTM and HyperGRU decrease the RMSE by 3.94% and 3.82% averaged on the air quality dataset; and 2.60% and 2.60% on the electricity consumption dataset. HyperGRU also outperforms ADARNN by increasing ACC by 1.32% and F1 score by 1.04% on the human activity dataset. These results

TABLE II
PERFORMANCE OF AIR QUALITY AND ELECTRICITY CONSUMPTION.

Methods	Dongsi		Tiantan		Nongzhanguan		Dingling		Electric Power RMSE
	RMSE	MAE	RMSE	MAE	RMSE	MAE	RMSE	MAE	
LSTM	0.0502	0.0403	0.0511	0.0453	0.0341	0.0476	0.0329	0.0339	0.092
GRU	0.0510	0.0380	0.0519	0.0475	0.0348	0.0459	0.0330	0.0347	0.093
LSTNet	0.0544	0.0651	0.0519	0.0651	0.0548	0.0696	0.0599	0.0705	0.080
MMD-RNN	0.0360	0.0267	0.0183	0.0133	0.0267	0.0197	0.0288	0.0168	0.082
DANN-RNN	0.0356	0.0255	0.0214	0.0157	0.0274	0.0203	0.0291	0.0211	0.080
STRIPE	0.0365	0.0216	0.0204	0.0148	0.0248	0.0154	0.0304	0.0139	0.086
ADARNN	0.0295	0.0185	0.0164	0.0112	0.0196	0.0122	0.0233	0.0150	0.077
HyperLSTM	0.0278	0.0178	0.0155	0.0107	0.0189	0.0120	0.0231	0.0134	0.075
HyperGRU	0.0285	0.0182	0.0156	0.0111	0.0184	0.0119	0.0229	0.0138	0.075

TABLE III
PERFORMANCE OF HUMAN ACTIVITY PREDICTION

Methods	ACC	P	R	F1
LightGBM	84.11	83.73	83.63	84.91
GRU	85.68	85.62	85.51	85.46
MMD-RNN	86.39	86.80	86.26	86.38
DANN-RNN	85.88	85.59	85.62	85.56
ADARNN	88.44	88.71	88.59	88.63
HyperGRU	89.61	89.64	89.45	89.43

indicate that HTSF can better characterize the distribution shifts in data.

B. Grid-based Spatiotemporal Forecasting

In this subsection, we demonstrate the applicability of HTSF to spatiotemporal data (grid-based). We are interested in the gains by explicitly accounting for the distribution shifts in spatiotemporal data forecasting.

1) *Datasets and Metrics.*: We experiment with NYC-Taxi and NYC-Bike, two datasets of trip records collected in New York City (NYC) with grid partitioned regions for traffic prediction. NYC-Taxi contains taxi trip records of NYC from 01/01/2015 to 03/01/2015. NYC-Bike contains bike trip records of NYC from 07/01/2016 to 08/29/2016. For both datasets, The first 40 days are used as the training set. We use the Mean Absolute Percentage Error (MAPE) and RMSE as the performance metrics.

2) *Baselines and Configurations.*: A mainstream strategy to process spatiotemporal data with grid partition is to combine CNNs and RNNs [38], [39]. We choose three representative methods adopting this strategy as the baselines.

- **ConvLSTM** [35]: an extension of LSTM using convolution operators to build cells.
- **DMVST-Net** [38]: it combines CNN and LSTM in a joint model that captures the complex relations from both spatial and temporal perspectives.
- **STDN** [39]: it designs a periodically shifted attention mechanism to capture long-term dependency and applies LSTM to learn short-term dependency.

We pick these three methods because ConvLSTM is one of the earliest deep learning models for grid-based spatiotemporal data analysis, while DMVST-Net and STDN are very strong baselines for NYC-Taxi and NYC-Bike.

TABLE IV
HTSF ADAPTED FOR GRID-BASED URBAN TRAFFIC PREDICTION.

Dataset	Method	pick-up		drop-off	
		RMSE	MAPE	RMSE	MAPE
NYC-Taxi	ConvLSTM	28.13	20.50	23.67	20.70
	DMVST-Net	25.74	17.38	20.51	17.14
	STDN	24.10	16.30	19.05	16.25
	HyperConvLSTM	26.45	19.41	22.15	29.64
	DMVST-Net w/HTSF	24.26	16.59	19.13	16.53
	STDN w/HTSF	23.26	15.74	18.53	16.26
NYC-Bike	ConvLSTM	10.40	25.10	9.22	23.20
	DMVST-Net	9.14	22.20	8.50	21.56
	STDN	8.85	21.84	8.15	20.87
	HyperConvLSTM	9.73	24.33	8.64	21.82
	DMVST-Net w/HTSF	8.66	21.51	7.97	20.45
	STDN w/HTSF	8.13	21.23	7.62	19.97

We adapt HTSF to spatiotemporal forecasting as follows.

- We adopt ConvLSTM as both the hyper layers and main layers to build the hypernetwork-based model for ConvLSTM, which we term HyperConvLSTM.
- Extensions to STDN and DMVST-Net are more challenging because STDN and DMVST-Net have dedicated components to learn spatial patterns, while HTSF is designed only to learn temporal patterns. Therefore, we reuse the corresponding spatial components in STDN and DMVST-Net but replace their temporal components with HyperLSTM. The corresponding models are termed STDN w/ HyperLSTM and DMVST-Net w/ HyperLSTM.

The region is split into 10×20 grids with size $1km \times 1km$. The Min-Max normalization is used to convert data value to the $[0, 1]$ scale. The time interval is set as half-hour. We set the sliding window size $T = 1344$ (four weeks), and $k = 48$ for 1D average pooling. L2 loss is used for training. We optimize all the models by Adam, and the learning rate is set to $2e-4$ with a weight decay of 0.01.

3) *Results.*: Table IV lists the results of traffic flow prediction on NYC-Taxi and NYC-Bike. We make the following observations.

- The best performance is achieved with HTSF, indicating the benefit of mitigating distribution shift in traffic prediction.
- For the three baselines, the corresponding hypernetwork-based architecture reduces the pick-up RMSE by 3.49%

TABLE V
DATASET DESCRIPTION OF PEMSD.

Datasets	#Detectors	Range
PeMSD3	358	9/1/2018-11/30/2018
PeMSD4	307	1/1/2018-2/28/2018
PeMSD7	883	5/1/2017-8/31/2017
PeMSD8	170	7/1/2016-8/31/2016

to 6.27% on NYC-Taxi and 5.54% to 8.13% on NYC-Bike; and reduces the drop-off RMSE by 2.73% to 6.73% on NYC-Taxi and 6.23% to 6.50% on NYC-Bike. Therefore, our hypernetwork-based framework is easily applicable in grid-based spatiotemporal data forecasting and notably improves prediction accuracy.

C. Graph-based Spatiotemporal Forecasting

Since graph neural network (GNN) based models have achieved the state-of-the-art performance in urban traffic forecasting [18], [19], we are interested in whether HTSF can further improve the performance of GNN-based models.

1) *Datasets and Metrics.*: We conduct experiments on PeMSD3, PeMSD4, PeMSD7, and PeMSD8, which are graph-based traffic datasets collected by the Caltrans Performance Measurement System [40] for traffic flow prediction. All the datasets are split with a ratio of 6:2:2 for training, validation, and testing. The traffic flows are aggregated into 5-minute interval. Table V summarizes the detailed information of the datasets. RMSE, MAE, and MAPE are used as performance metrics.

2) *Baselines and Configurations.*: We use the baselines below.

- **DCRNN** [41]: an extension of RNN using graph convolutional operators to build cells.
- **STGCN** [42]: it formulates traffic forecasting on graphs and builds the model with GCNs.
- **ASTGCN** [43]: an attention based spatiotemporal GCN, which can effectively model the dynamic spatiotemporal correlations in traffic data.
- **GraphWaveNet** [44]: it can capture the hidden spatial dependency via a novel adaptive dependency matrix.
- **AGCRN** [18]: an adaptive graph convolutional recurrent network to capture spatial and temporal correlations.
- **STFGNN** [19]: a spatiotemporal fusion GNN, which can effectively learn hidden spatiotemporal patterns by a fusion operation of various spatial and temporal graphs.

The selected GNN-based models include representative ([41], [42]) and state-of-the-art ([18], [19]) models for traffic forecasting.

We compare these methods with our HTSF using pure RNN-based models (HyperLSTM and HyperGRU) and an extension of HTSF to AGCRN, a GNN-based model. Specifically, we adopt AGCRN as the hyper layers and main layers to HTSF, and the corresponding model is termed HyperAGCRN. For all four datasets, we use the data of past 12 steps to predict the future

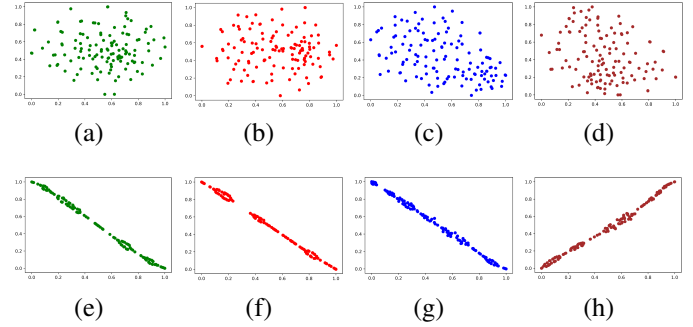


Fig. 3. Visualization of distribution shifts in the Air Quality dataset. The upperparts (a, b, c, d) present the original distribution visualization of four stations (Dongsi, Tiantan, Nongzhanguan, Dingling). The lower parts (e, f, g, h) present the learned distribution visualization of four stations (Dongsi, Tiantan, Nongzhanguan, Dingling). One scatter presents a sequence in S .

12 steps. We set sliding window size $T = 2016$ (one week), and $k = 24$ for 1D average pooling. We optimize all the models by Adam with batch size 128. The learning rate is set to $3e-4$ with a weight decay of 0.01.

3) *Results.*: Table VI summarizes the average results on graph-based spatiotemporal forecasting. We have the following observations.

- GNN-based models outperform LSTM and GRU since GNN-based models take advantage of modeling spatial patterns while LSTM and GRU only model the temporal patterns.
- Our HyperLSTM and HyperGRU, despite modeling only the temporal patterns, outperform multiple GNN-based models. For example, HyperLSTM and HyperLSTM have better RMSE, MAE, and MAPE than GraphWaveNet on PeMSD3, PeMSD4, and PeMSD7. The reason might be that the temporal distribution shift may be a more important bottleneck than the spatial patterns in the accuracy of traffic prediction.
- HyperAGCRN achieves the best performance across all datasets. This demonstrates that HTSF can improve the performance of GNN-based models.

VI. ABLATION STUDIES

A. Visual Analysis of Distribution Shift

1) *Setups.*: In this study, we demonstrate the problem of distribution shift in time series via visual analysis of the Air Quality dataset. For each station, we randomly sample one instance $\mathbf{x}^{(i)}$ with its corresponding historical dataset $S = \{\hat{\mathbf{x}}_n^{(i)}\}_{n=1}^L$, where S contains 128 sequences, *i.e.*, $L = 128$. We use t-SNE [45] to visualize the learned distributions (via the hyper layers) of all sequences in S and their original distributions.

2) *Results.*: From Figure 3, we observe that the original distributions are random while the learned distributions can be approximately fitted by a linear model, indicating that common knowledge among all historical sequences has been learned by HTSF.

TABLE VI
HTSF ADAPTED FOR GRAPH-BASED TRAFFIC PREDICTION.

Methods	PeMSD3			PeMSD4			PeMSD7			PeMSD8		
	RMSE	MAE	MAPE	RMSE	MAE	MAPE	RMSE	MAE	MAPE	RMSE	MAE	MAPE
LSTM	35.11	21.33	21.33	39.59	25.14	20.33	42.84	29.98	15.33	32.06	22.20	15.32
GRU	36.23	21.47	21.06	38.87	25.36	20.49	41.93	30.14	15.71	32.24	23.03	15.62
DCRNN	30.31	18.18	18.91	38.12	24.70	17.12	38.58	28.30	11.66	27.83	17.86	11.45
STGCN	30.12	17.49	17.15	35.55	22.70	14.59	38.78	25.38	11.08	27.83	18.02	11.40
ASTGCN	29.66	17.69	19.40	35.22	22.93	16.56	42.57	28.05	13.92	28.16	18.61	13.08
GraphWaveNet	32.94	19.85	19.31	39.70	25.45	17.29	42.78	26.85	12.12	31.05	19.13	12.68
AGCRN	-	-	-	32.30	19.83	12.97	-	-	-	25.22	15.95	10.09
STFGNN	26.28	16.77	16.30	32.51	20.48	16.77	36.60	23.46	9.21	26.25	16.94	10.60
HyperLSTM	32.36	19.21	19.04	37.19	23.65	18.46	38.67	27.18	13.17	28.12	19.20	13.68
HyperGRU	32.18	19.42	18.79	36.94	23.47	19.14	38.75	27.31	12.73	27.84	19.33	14.23
HyperAGCRN	25.68	15.85	14.37	29.93	18.89	12.11	34.37	21.64	8.89	24.37	15.26	9.64

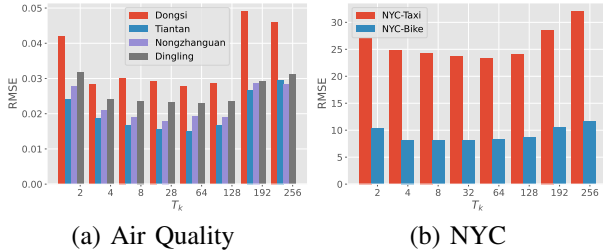


Fig. 4. Impact of sliding window size T on the forecasting accuracy.

B. Impact of Sliding Window Length

1) *Setups*: The length of the sliding window T is an important hyper-parameter in HTSF. We experiment with different lengths using HyperGRU on the datasets of Air Quality, NYC-Taxi and NYC-Bike. As mentioned in Sec. IV-B, the actual input length of the hyper layers is $\frac{T}{k}$. Let $T_k = \frac{T}{k}$, to observe how sensitive the model is to T_k , we vary T_k from 2 to 256. Length 2 is the shortest length of a sequence, and Length 256 is challenging for optimization of GRU.

2) *Results*: Figure 4 plots the performance variations of HyperGRU on Air-quality, NYC-Taxi and NYC-Bike as the sliding window length increases. We observe high error (in RMSE) when $T_k = 2$. One potential reason may be that it is difficult to learn complex feature representations of the distribution shifts given very short sequences. The RMSE only experiences a small variance when T_k increases from 4 to 128. When $T_k \geq 192$, the RMSE starts to grow again. One potential reason is that when considering a very long length, the training becomes harder. This results show that HTSF is insensitive to sliding window length, except in extreme cases ($T_k = 2$ or $T_k \geq 192$).

C. Impact of Prediction Horizon

1) *Setups*: Multi-step prediction capability is crucial for traffic flow forecasting. We analyze the performance of HyperGRU for multi-step prediction on PeMSD4 and PeMSD8 datasets.

2) *Results*: Figure 5 shows the prediction performance of various methods as the horizon increases. Overall, the errors (in MAE) grow with the forecast step. However, for both

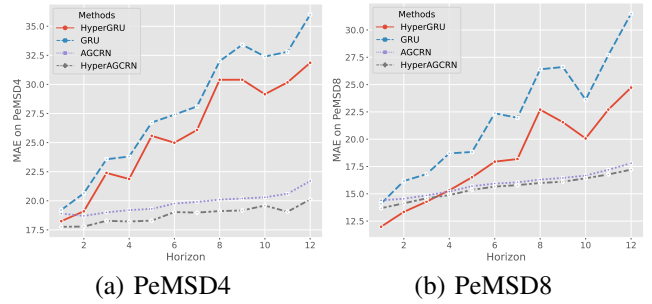


Fig. 5. Multi-step prediction performance on PeMSD.

datasets, the errors of AGCRN and HyperAGCRN increase much more slowly than GRU and HyperGRU. HTSF significantly improves the performance of GRU and HyperAGCRN on multi-step prediction, while our HyperAGCRN achieves the best results for all horizons. These results indicate that mitigating the distribution shift problem using HTSF is effective in mining the dynamic patterns of spatiotemporal data.

VII. CONCLUSION

In this paper, we investigate the distribution shift problem in the time series forecasting problem, which causes discrepancies between the distributions of the training and the testing data. To this end, we propose HTSF, a novel hypernetwork-based framework which applies for time series forecasting under distribution shift. Specifically, HTSF exploits the hyper layers to learn the best characterization of the distribution shifts, generating the model parameters for the main layers to make accurate predictions. Moreover, HTSF is implemented as an extensible framework that can incorporate diverse time series forecasting models such as RNNs and Transformers. Extensive experiments show that HTSF outperforms other state-of-the-art methods on 9 benchmarks.

REFERENCES

- [1] S. Zhang, B. Guo, A. Dong, J. He, Z. Xu, and S. X. Chen, "Cautionary tales on air-quality improvement in beijing," *Proceedings of the Royal Society A: Mathematical, Physical and Engineering Sciences*, vol. 473, no. 2205, p. 20170457, 2017.
- [2] D. Lee and K. Kim, "Recurrent neural network-based hourly prediction of photovoltaic power output using meteorological information," *Energies*, vol. 12, no. 2, pp. 1–22, 2019.
- [3] B. Almaslukh, J. AlMuhtadi, and A. Artoli, "An effective deep autoencoder approach for online smartphone-based human activity recognition," *Int. J. Comput. Sci. Netw. Secur.*, vol. 17, no. 4, pp. 160–165, 2017.
- [4] H. Zhou, S. Zhang, J. Peng, S. Zhang, J. Li, H. Xiong, and W. Zhang, "Informer: Beyond efficient transformer for long sequence time-series forecasting," in *Proceedings of the AAAI Conference on Artificial Intelligence*. Palo Alto, CA, USA: AAAI Press, 2021, pp. 11 106–11 115.
- [5] J. D. Hamilton, *Time series analysis*. Princeton, NJ, USA: Princeton university press, 2020.
- [6] J. Connor, L. E. Atlas, and D. R. Martin, "Recurrent networks and narma modeling," in *Advances in Neural Information Processing Systems*. Red Hook, NY, USA: Curran Associates Inc., 1992, pp. 301–308.
- [7] A. Vaswani, N. Shazeer, N. Parmar, J. Uszkoreit, L. Jones, A. N. Gomez, L. Kaiser, and I. Polosukhin, "Attention is all you need," in *Advances in Neural Information Processing Systems*. Red Hook, NY, USA: Curran Associates Inc., 2017, pp. 6000–6010.
- [8] G. Lai, W.-C. Chang, Y. Yang, and H. Liu, "Modeling long-and short-term temporal patterns with deep neural networks," in *Proceedings of the International SIGIR Conference on Research & Development in Information Retrieval*. New York, NY, USA: ACM, 2018, pp. 95–104.
- [9] V. Le Guen and N. Thome, "Probabilistic time series forecasting with structured shape and temporal diversity," in *Advances in Neural Information Processing Systems*. Red Hook, NY, USA: Curran Associates Inc., 2020, pp. 4427–4440.
- [10] D. Salinas, V. Flunkert, J. Gasthaus, and T. Januschowski, "Deepar: Probabilistic forecasting with autoregressive recurrent networks," *International Journal of Forecasting*, vol. 36, no. 3, pp. 1181–1191, 2020.
- [11] V. Kuznetsov and M. Mohri, "Generalization bounds for time series prediction with non-stationary processes," in *Proceedings of the International Conference on Algorithmic Learning Theory*. Berlin, Germany: Springer, 2014, pp. 260–274.
- [12] Y. Du, J. Wang, W. Feng, S. Pan, T. Qin, and C. Wang, "Adarnn - adaptive learning and forecasting of time series," in *Proceedings of the International Conference on Information and Knowledge Management*. New York, NY, USA: ACM, 2021, pp. 402–411.
- [13] A. Torralba and A. A. Efros, "Unbiased look at dataset bias," in *Proceedings of the Conference on Computer Vision and Pattern Recognition*. Piscataway, NJ, USA: IEEE Press, 2011, pp. 1521–1528.
- [14] E. Tzeng, J. Hoffman, K. Saenko, and T. Darrell, "Adversarial discriminative domain adaptation," in *Proceedings of the Conference on Computer Vision and Pattern Recognition*. Piscataway, NJ, USA: IEEE Press, 2017, pp. 2962–2971.
- [15] J. Wang, C. Lan, C. Liu, Y. Ouyang, and T. Qin, "Generalizing to unseen domains: A survey on domain generalization," in *Proceedings of the International Joint Conference on Artificial Intelligence*. Burlington, MA, USA: Morgan Kaufmann, 2021, pp. 4627–4635.
- [16] J. Wang, W. Feng, Y. Chen, H. Yu, M. Huang, and P. S. Yu, "Visual domain adaptation with manifold embedded distribution alignment," in *Proceedings of the International Conference on Multimedia*. New York, NY, USA: ACM, 2018, pp. 402–410.
- [17] T. Kim, J. Kim, Y. Tae, C. Park, J.-H. Choi, and J. Choo, "Reversible instance normalization for accurate time-series forecasting against distribution shift," *Proceedings of the International Conference on Learning Representations*, 2022.
- [18] L. Bai, L. Y. and Can Li, X. Wang, and C. Wang, "Adaptive graph convolutional recurrent network for traffic forecasting," in *Advances in Neural Information Processing Systems*. Red Hook, NY, USA: Curran Associates Inc., 2020, pp. 17 804–17 815.
- [19] M. Li and Z. Zhu, "Spatial-temporal fusion graph neural networks for traffic flow forecasting," in *Proceedings of the AAAI Conference on Artificial Intelligence*. Palo Alto, CA, USA: AAAI Press, 2021, pp. 4189–4196.
- [20] P. J. Brockwell, R. A. Davis, J. O. Berger, S. E. Fienberg, and B. Singer, *Time Series: Theory and Methods*. Berlin, Germany: Springer, 1987.
- [21] A. A. Ariyo, A. O. Adewumi, and C. K. Ayo, "Stock price prediction using the ARIMA model," in *Proceedings of the International Conference on Computer Modelling and Simulation*. Piscataway, NJ, USA: IEEE Press, 2014, pp. 106–112.
- [22] V. Le Guen and N. Thome, "Shape and time distortion loss for training deep time series forecasting models," in *Advances in Neural Information Processing Systems*. Red Hook, NY, USA: Curran Associates Inc., 2019, pp. 4189–4201.
- [23] S. Li, X. Jin, Y. Xuan, X. Zhou, W. Chen, Y.-X. Wang, and X. Yan, "Enhancing the locality and breaking the memory bottleneck of transformer on time series forecasting," in *Advances in Neural Information Processing Systems*. Red Hook, NY, USA: Curran Associates Inc., 2019, pp. 5243–5253.
- [24] J. Jiang, Y. Ji, X. Wang, Y. Liu, J. Wang, and M. Long, "Regressive domain adaptation for unsupervised keypoint detection," in *Proceedings of the Conference on Computer Vision and Pattern Recognition*. Piscataway, NJ, USA: IEEE Press, 2021, pp. 6776–6785.
- [25] D. Ha, A. M. Dai, and Q. V. Le, "Hypernetworks," *Proceedings of the International Conference on Learning Representations*, 2017.
- [26] C. Zhang, M. Ren, and R. Urtasun, "Graph hypernetworks for neural architecture search," *Proceedings of the International Conference on Learning Representations*, 2019.
- [27] J. von Oswald, C. Henning, J. Sacramento, and B. F. Grewe, "Continual learning with hypernetworks," *Proceedings of the International Conference on Learning Representations*, 2020.
- [28] T. Galanti and L. Wolf, "On the modularity of hypernetworks," in *Advances in Neural Information Processing Systems*. Red Hook, NY, USA: Curran Associates Inc., 2020, pp. 10 409–10 419.
- [29] L. Bertinetto, J. F. Henriques, J. Valmadre, P. Torr, and A. Vedaldi, "Learning feed-forward one-shot learners," in *Advances in Neural Information Processing Systems*. Red Hook, NY, USA: Curran Associates Inc., 2016, pp. 523–531.
- [30] R. K. Mahabadi, S. Ruder, M. Dehghani, and J. Henderson, "Parameter-efficient multi-task fine-tuning for transformers via shared hypernetworks," in *Proceedings of the Annual Meeting of the Association for Computational Linguistics*. Stroudsburg, PA, USA: ACL, 2021, pp. 565–576.
- [31] W. Duan, X. He, Z. Zhou, H. Rao, and L. Thiele, "Injecting descriptive meta-information into pre-trained language models with hypernetworks," in *Proceedings of the Conference of the International Speech Communication Association*. ISCA, 2021, pp. 3216–3220.
- [32] Z. Pan, Y. Liang, W. Wang, Y. Yu, Y. Zheng, and J. Zhang, "Urban traffic prediction from spatio-temporal data using deep meta learning," in *Proceedings of the SIGKDD International Conference on Knowledge Discovery & Data Mining*. New York, NY, USA: ACM, 2019, pp. 1720–1730.
- [33] M.-T. Luong, H. Pham, and C. D. Manning, "Effective approaches to attention-based neural machine translation," *arXiv preprint arXiv:1508.04025*, 2015.
- [34] S. Hochreiter and J. Schmidhuber, "Long short-term memory," *Neural Computation*, vol. 9, no. 8, pp. 1735–1780, 1997.
- [35] X. Shi, Z. Chen, H. Wang, D. Yeung, W. Wong, and W. Woo, "Convolutional LSTM network: A machine learning approach for precipitation nowcasting," in *Advances in Neural Information Processing Systems*. Red Hook, NY, USA: Curran Associates Inc., 2015, pp. 802–810.
- [36] Kaggle, "Household electric power consumption dataset," <https://www.kaggle.com/uciml/electric-power-consumption-data-set>, 2021.
- [37] D. P. Kingma and J. Ba, "Adam: A method for stochastic optimization," *Proceedings of the International Conference on Learning Representations*, 2015.
- [38] H. Yao, F. Wu, J. Ke, X. Tang, Y. Jia, S. Lu, P. Gong, J. Ye, and Z. Li, "Deep multi-view spatial-temporal network for taxi demand prediction," in *Proceedings of the AAAI Conference on Artificial Intelligence*. Palo Alto, CA, USA: AAAI Press, 2018, pp. 2588–2595.
- [39] H. Yao, X. Tang, H. Wei, G. Zheng, and Z. Li, "Revisiting spatial-temporal similarity: A deep learning framework for traffic prediction," in *Proceedings of the AAAI Conference on Artificial Intelligence*. Palo Alto, CA, USA: AAAI Press, 2019, pp. 5668–5675.
- [40] C. Chen, K. Petty, A. Skabardonis, P. Varaiya, and Z. Jia, "Freeway performance measurement system: Mining loop detector data," *Transportation Research Record*, vol. 1748, no. 1, pp. 96–102, 2001.

- [41] Y. Li, R. Yu, C. Shahabi, and Y. Liu, "Diffusion convolutional recurrent neural network: Data-driven traffic forecasting," *Proceedings of the International Conference on Learning Representations*, 2018.
- [42] B. Yu, H. Yin, and Z. Zhu, "Spatio-temporal graph convolutional networks: A deep learning framework for traffic forecasting," in *Proceedings of the International Joint Conference on Artificial Intelligence*. Burlington, MA, USA: Morgan Kaufmann, 2018, pp. 3634–3640.
- [43] S. Guo, Y. Lin, N. Feng, C. Song, and H. Wan, "Attention based spatial-temporal graph convolutional networks for traffic flow forecasting," in *Proceedings of the AAAI Conference on Artificial Intelligence*. Palo Alto, CA, USA: AAAI Press, 2019, pp. 922–929.
- [44] Z. Wu, S. Pan, G. Long, J. Jiang, and C. Zhang, "Graph wavenet for deep spatial-temporal graph modeling," in *Proceedings of the International Joint Conference on Artificial Intelligence*. Burlington, MA, USA: Morgan Kaufmann, 2019, pp. 1907–1913.
- [45] V. D. M. Laurens and G. Hinton, "Visualizing data using t-sne," *Journal of Machine Learning Research*, vol. 9, no. 2605, pp. 2579–2605, 2008.